Development 117, 977-991 (1993)
Printed in Great Britain © The Company of Biologists Limited 1993

A functionally specialized α-tubulin is required for oocyte meiosis and cleavage mitoses in *Drosophila*

Kathleen A. Matthews*, Dianne Rees and Thomas C. Kaufman

Department of Biology, Indiana University, Bloomington, IN 47405, USA

*Author for correspondence

SUMMARY

Three α-tubulin proteins contribute to microtubules during oogenesis and early embryogenesis in *Drosophila melanogaster*: αTUB84B, αTUB84D, and αTUB67C. αTUB67C is unique in two respects. It is a structurally divergent α-tubulin, sharing only 67% amino acid identity with the generic isotypes αTUB84B and αTUB84D, and its expression is exclusively maternal. The genetic analysis of the α*Tub67C* gene described here demonstrates that αTUB67C is required for nuclear division in the oocyte and early embryo. Both meiosis and cleavage-stage mitoses are severely affected by mutations that result in a substantial decrease in the ratio of αTUB67C/αTUB84B+αTUB84D. A large increase in this ratio, achieved by increasing the gene dosage of α*Tub67C*, has little or no effect on meiosis, but severely disrupts mitotic spindle function. Thus, both classes of α-tubulin isotype present in the mature oocyte, αTUB67C and αTUB84B/84D, are essential for normal spindle function in early *Drosophila* development. These α-tubulins provide the first example of tubulin isotypes known to be coexpressed in wild-type animals whose encoded variation is required for the normal function of a microtubule array.

Key words: tubulin, isotype, regulation, meiosis, mitosis, spindles, *Drosophila*

INTRODUCTION

Morphogenesis requires the microtubule cytoskeleton to undergo continual restructuring in response to developmental programs. Microtubule assembly and disassembly is coordinated to ensure the orderly progression of meiotic and mitotic divisions, cell shape changes, and cellular and subcellular movements. The wide range of dynamic properties associated with different microtubule populations (Cassimeris et al., 1988; Horio and Hotani, 1986; Okabe and Hirokawa, 1990; Walker et al., 1990) requires spatial and temporal regulation of the stability of specific microtubule classes. An understanding of the cellular mechanisms involved in regulating microtubule function will be an important addition to our knowledge of development.

The control of microtubule behavior is likely to be governed both by the basic components of the microtubule, the α- and β-tubulins, and the proteins that interact with microtubules. Microtubule-associated proteins (MAPs) have been shown to have a significant effect on microtubule dynamics (Cleveland et al., 1977; Drubin and Kirschner, 1986; Lewis et al., 1989). The role of tubulin heterogeneity in influencing microtubule assembly is less clear. In all but the simplest eukaryotes, α- and β-tubulins are encoded by small multigene families. These families typically consist of a highly conserved, essentially universally expressed tubulin and a number of variant isotypes which may be subject to tissue- or stage-specific regulation. Microtubules are typically copolymers of the tubulin isotypes available at the time of assembly (Bond et al., 1986; Lewis et al., 1987; Lopata and Cleveland, 1987; Baker et al., 1990; Theurkauf, 1992).

The great majority of tubulin isotypes tested for functional specificity have proved to be multifunctional (Bond et al., 1986; Joshi et al., 1987; Lewis et al., 1987; Schatz et al., 1986). However, at least one functionally specialized tubulin variant has been identified. The divergent β3-tubulin isotype of *Drosophila*, when misexpressed in the male germ line in the absence of the normal β2 isotype, is capable of supporting only one of the several classes of microtubule arrays required for the post-mitotic stages of spermatogenesis (Hoyle and Raff, 1990). With normal pools of β2-tubulin, the β3 isotype poisons axoneme assembly when the ratio of β3/β2 exceeds 20%. Indirect but intriguing evidence for an array-specific isotype is provided by the *mec-7* β-tubulin gene in *Caenorhabditis elegans* (Savage et al., 1989). Touch insensitive mutations in *mec-7* disrupt production of the 15-protofilament microtubules that characterize touch-receptor neurons in these animals without apparent effect on 11-protofilament-microtubule-mediated functions. Thus, the widespread occurrence of multiple tubulin isotypes in eukaryotes presumably reflects their utility in both regulating tubulin production and supporting exceptional functional characteristics of certain microtubule arrays (Raff, 1984).

The α-tubulin gene family in *Drosophila* (Kalfayan and

Wensink, 1981, 1982; Mischke and Pardue, 1982; Theurkauf et al., 1986; Matthews et al., 1989) provides a useful system in which to examine the contribution of tubulin variation to microtubule specialization during development. This family contains four encoded isotypes which display varying degrees of temporal and spatial regulation (Kalfayan and Wensink, 1982; Matthews et al., 1989, 1990; Bo and Wensink, 1989). Two of the α-tubulins, αTUB84B and αTUB84D, differing by only two amino acids (Theurkauf et al., 1986), are expressed in most tissues throughout development (Kalfayan and Wensink, 1982; Matthews et al., 1989) and are very similar in sequence to abundant α-tubulins from distantly related organisms (Theurkauf et al., 1986). αTUB85E, 5% diverged from αTUB84B (Theurkauf et al., 1986), is the only nonmaternal α-tubulin in *Drosophila* and its accumulation is restricted to a few classes of morphologically similar but lineally unrelated cells (Bo and Wensink, 1989; Matthews et al., 1990). αTUB67C is the most divergent α-tubulin yet identified, sharing only 67% amino acid identity with αTUB84B (Theurkauf et al., 1986). Expression of αTUB67C is restricted to the ovary, accounting for 20% or more of the α-tubulin in a mature egg (Matthews et al., 1989). In the embryo, αTUB67C and αTUB84B/84D coassemble into all classes of microtubules present through cellular blastoderm formation (Theurkauf, 1992).

We have examined the role of α*Tub67C* in early embryonic development by altering the normal contribution of αTUB67C to the tubulin pool of oocytes and therefore early embryos. Reduction in the pool of functional αTUB67C disrupts both meiotic and mitotic spindle function. Excess αTUB67C produced from transgenic copies of α*Tub67C* has little or no effect on meiosis, but disrupts cleavage, an effect that is counteracted by simultaneously increasing the dosage of α*Tub84B*. Our results indicate that some aspect(s) of the structural difference between αTUB67C and αTUB84B/84D are indeed crucial to microtubule function during early *Drosophila* development. α-Tubulin isotypes of the *Drosophila* oocyte thus provide the first example of normally coexpressed tubulins with distinctive functional properties.

MATERIALS AND METHODS

Screens for mutations

Flies were raised at 24-25°C on standard cornmeal-agar-molasses medium. Visible mutations and balancers are described in Lindsley and Zimm (1992).

α*Tub67C* mutations were recovered in three ways. Isogeneic *ri e* males were mutagenized with 25 mM ethyl methane sulfonate (EMS) according to the procedure of Lewis and Bacher (1968) and mated to *TM3/TM6B* virgin females. Individual *ri e/TM3* or *ri e/TM6B* male progeny were mated to three *Df(3L)AC1/TM3* virgin females. From each cross, a temporary stock was established from *ri e/TM3* males and females, and *ri e/Df(3L)AC1* females were tested for fertility. 8,750 chromosomes were screened for EMS-induced mutations. A second screen of 3,000 chromosomes followed the same mating and testing protocol, but *ri e* males were mutagenized with 3000 rads of X-irradiation instead of EMS. A third screen used 60 mM diepoxy butane as a mutagen, according to the procedure of Leicht and Bonner (1988), and tested 4,000 mutagenized chromosomes for the ability to complement an α*Tub67C* mutation recovered in the EMS screen (α$Tub67C^2$).

Fertility assays and effective lethal phase determinations

Fertility tests measured the proportion of eggs produced by females of a given genotype that hatched, producing first instar larvae. In most cases, viability to adult was also monitored. Virgin females were mated to males for 24-72 hours prior to the first collection of eggs. Collections were made for up to 16 hours on soft-agar plates. Eggs were then picked and placed on hard agar plates (100-200 eggs per plate) that had a blob of yeast paste on the surface, away from the rows of eggs. The unhatched eggs were scored not less than 30 hours after the end of the egg collection. First instar larvae crawl to the yeast paste, leaving the unhatched eggs largely undisturbed.

Transformation vectors and complementation crosses

A genomic clone of the α*Tub67C* gene (Kalfayan and Wensink, 1981) was kindly provided by P. C. Wensink. A 7 kb *Bam*HI genomic fragment containing the α*Tub67C* coding sequences plus 1.5 kb upstream of the initiation site and 3 kb downstream of the polyadenylation site (Theurkauf et al., 1986) was cloned into CaSpeR (Pirrotta, 1988). A replica of the developmental northern blot shown in Matthews et al. (1989) was probed with the 7 kb *Bam*HI fragment to test for the presence of genes other than α*Tub67C*. In addition to α*Tub67C* mRNA, the 7 kb fragment identified a testis-specific mRNA. Thus, although at least part of another gene is included in this construct, it's domain of expression does not detectably overlap with that of α*Tub67C* and should not have a confounding effect on the interpretation of rescue experiments involving female sterile mutations. Germ-line transformations were carried out as described by Robertson et al., 1988.

Two independent α*Tub67C* transformant lines, both with inserts on the second chromosome, were used for initial complementation tests with female sterile mutations. Females of the genotype *w*; *P{*w^+ α$Tub67C^+$*}i*/+; *fs*/*Df(3L)AC1* (where *fs* denotes the female sterile mutation being tested) were examined for the production and viability of eggs. Rescued alleles showed from 50% embryonic viability (α$Tub67C^1$) to 96% embryonic viability (α$Tub67C^3$).

A genomic clone of the α*Tub84B* gene (Kalfayan and Wensink, 1981; Mischke and Pardue, 1982) was kindly provided by M. L. Pardue. The α*Tub84B* transformation vector was constructed by cloning a 4.5 kb *Hin*dIII genomic fragment containing the α*Tub84B* coding sequences plus 1.7 kb upstream of the initiation site and 0.5 kb downstream of the polyadenylation site (Theurkauf et al., 1986) into the CaSpeR vector (Pirrotta, 1988). Germ-line transformations were carried out as described by Robertson et al., 1988.

Isotype-specific antibodies

A *Bst*N1-*Ava*II fragment from the genomic clone of α*Tub67C* was subcloned into the vector pWR590 (Guo et al., 1984) and expressed in *Escherishia coli* JM101. This fragment includes sequences for amino acids 32-63 of the αTUB67C protein, a region that contains no homology to any of the other α-tubulins. A *Hin*f fragment from a genomic clone of the α*Tub84B* gene was similarly subcloned and expressed. The resulting fusion protein contains amino acids 439-450 of α*Tub84B*; this sequence is identical in α*Tub84D*, but shares no more than two consecutive residues with α*Tub85E* and α*Tub67C*.

Crude protein fractions were obtained according to the proce-

dure of Diederich et al. (1989) and partial purification of the fusion proteins was as described in Mahaffey and Kaufman (1987). Anti-αTUB67C and anti-αTUB84B/84D antibodies were affinity purified from rabbit immune sera after four boosts as described by Matthews et al. (1990). The resulting antibodies recognize only their respective isotypes on immunoblots of 2D gels (data not shown).

Immunoblots

Sample preparation, polyacrylamide gel electrophoresis, protein transfer, and antibody detection of proteins were performed as described by Matthews et al. (1989). The monoclonal mouse anti-α-tubulin used on immunoblots was purchased from Amersham and used at a 1:2500 dilution.

Immunohistochemistry

Eggs stained with anti-DNA were fixed as described by Matthews et al. (1990); those stained with any of the anti-tubulin antibodies were fixed according to the procedure of Warn and Warn (1986), with the following modifications. All procedures were carried out at room temperature. Following dechorionation as described by Matthews et al. (1990), buffer, methanol and heptane were added to the eggs, in that order. Tubes were shaken by hand throughout a 10 minute fixation period. Eggs that sank to the bottom of the tube were rinsed twice in 100% methanol, then rocked for 30 minutes in 1 ml of fresh methanol to which 10 μl of 30% hydrogen peroxide had been added. Eggs were then rinsed with methanol and stored at −20°C, or stained immediately. Ovaries were fixed according to the imaginal disc procedure of Pattatucci and Kaufman (1990).

Staining of both eggs and ovaries was carried out as described by Matthews et al. (1990), with substitution of the appropriate primary and secondary antibodies. All steps of the staining reactions were carried out in final volumes of 200 μl in 0.5 ml centrifuge tubes. The anti-DNA was a mouse monoclonal antibody purchased from Boehringer-Mannheim and used at 0.002 μg/μl. This antibody worked consistently well on eggs/embryos, but with the methods used here, penetration of developing follicles in ovaries was very poor. Sperm were identified with the mouse monoclonal antibody Ax-D5, the gift of Tim Karr, used without dilution (Karr, 1991).

RESULTS

Isolation of α*Tub67C* mutations

Mutations in the α*Tub67C* gene were recovered from screens for female sterile mutations in the interval 67A-67D, the region defined by the only deficiency available that removes the α*Tub67C* gene, *Df(3L)AC1*. Twenty-three mutations were recovered, defining maximally 7 complementation groups, one composed of 15 alleles, one of 3 alleles, and 5 of a single allele each. A transgenic copy of the α*Tub67C* gene was used to test the ability of wild-type αTUB67C to restore the fertility of females hemizygous for each of the 23 mutations. Only the mutations belonging to the three member complementation group were rescued by a wild-type α*Tub67C* gene. An additional α*Tub67C* allele was recovered by screening DEB-mutagenized chromosomes for the failure to complement the female sterility of one of the EMS-induced alleles.

To eliminate the possibility that mutations in other tubulin genes were represented in the α*Tub67C* complementation group (Matthews and Kaufman, 1987; Hays et al., 1989), the four mutations were mapped recombinationally. In all cases, the locus responsible for female sterility fell between *h* (66D15) and *th* (72B1) at 32.26±1.26 map units. α*Tub67C* is the only α-tubulin in the *h-th* interval (Kalfayan and Wensink, 1981; Mischke and Pardue, 1982). The four α*Tub67C* alleles are α*Tub67C*^{1} (EMS), α*Tub67C*^{2} (EMS), α*Tub67C*^{3} (X-ray), and α*Tub67C*^{4} (DEB).

α-tubulin pools in α*Tub67C* mutants

Accumulated pools of αTUB67C were examined on two-dimensional immunoblots of α*Tub67C*^{i}/*Df(3L)AC1* ovary and unfertilized egg proteins. Since there is no detectable synthesis of αTUB67C in embryos (Matthews et al., 1989, and unpublished observations), the pool of αTUB67C in mature eggs reflects the maximum amount available to the developing embryo. The only difference we have observed between the α-tubulin pools of unfertilized eggs and early embryos is the presence, in unfertilized eggs, of an additional lower apparent relative molecular mass protein that stains with the commercial monoclonal anti-α-tubulin antibody, but is not recognized by the αTUB67C-specific polyclonal antibody. The commercial antibody recognizes an epitope within the carboxy-25% of all four α-tubulins (Serrano et al., 1986, Theurkauf et al., 1986), while the polyclonal antibody recognizes an epitope between amino acids 32 and 62. We have never detected this protein in samples of any other stage/tissue of wild-type animals, but it does appear among proteins of pupae carrying a fusion gene that expresses αTUB67C from the α*Tub85E* promoter (our unpublished observations). These data suggest that the additional α-tubulin isoform found in unfertilized eggs is a proteolytic fragment of αTUB67C (lacking the amino 7-13% of the protein) that is stable in unfertilized eggs, but rapidly degrades in embryos.

As shown in Fig. 1, a small pool of intact mutant protein accumulates in ovaries and unfertilized eggs of *1/-* and *2/-* females. Ovaries from *3/-* females contain a pool of allele *3* protein comparable to that of +/+ females (after adjusting for dosage), but intact mutant protein in unfertilized eggs (Fig. 1, row 3) is barely detectable. We were unable to detect allele *4* protein on blots of any of the samples, but, as described below, mutant αTUB67C protein is detected in developing egg chambers when intact tissues are stained. In all cases, the vestigial pool of mutant αTUB67C protein in unfertilized eggs is accompanied by a corresponding increase in the pool of the putative proteolytic fragment of αTUB67C, suggesting that mutant protein is produced in approximately normal quantities but is less stable than wild-type protein.

Recessive phenotypes of α*Tub67C* mutations

The effective lethal phases of progeny of hemizygous and homozygous (where viable) mutant females are shown in Table 1. Essentially none of the eggs produced by hemizygous females hatch - a single first instar larva was observed among the 2,763 eggs scored for the four genotypes. Two percent of the eggs laid by *2/2* females supported development to adult and 0.6% of eggs from *1/2* females grew to adults; the remaining genotypes were completely sterile, with developmental arrest occurring almost exclusively in oocytes or embryos. Background lethal muta-

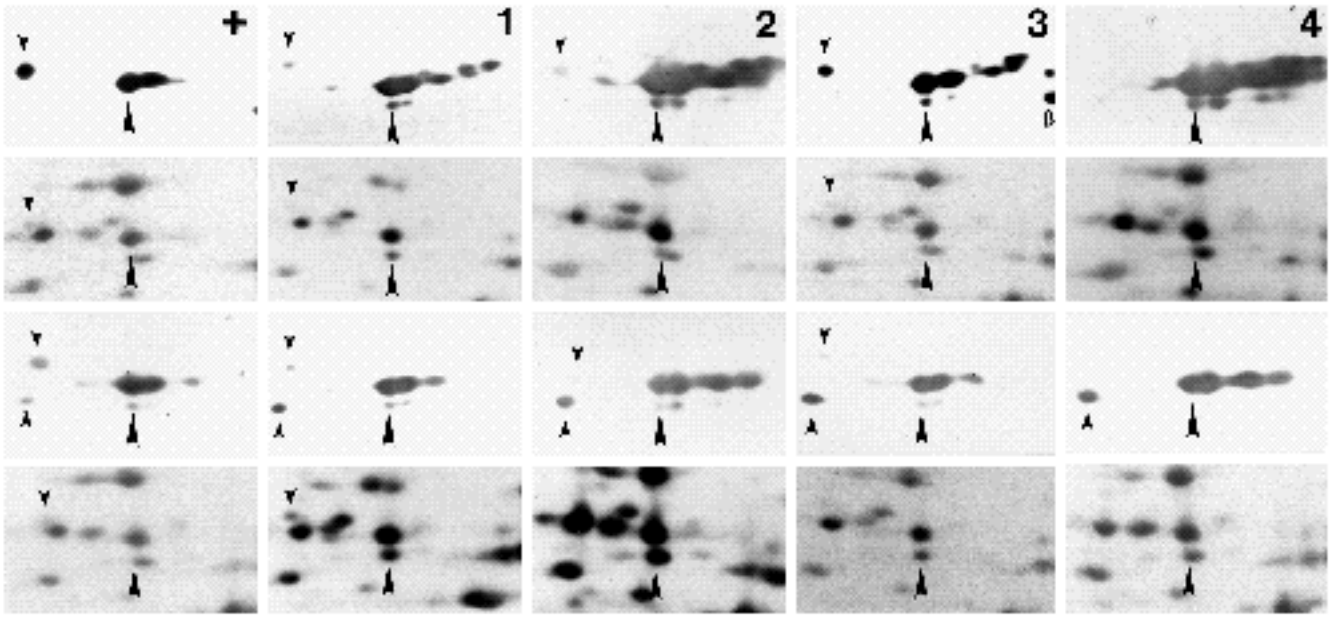

Fig. 1. αTUB67C synthesis and accumulation in α*Tub67C* mutations. Each column contains one genotype. + = Oregon-R; 1 = α*Tub67C*^{1}/-; 2 = α*Tub67C*^{2}/-; 3 = α*Tub67C*^{3}/-; 4 = α*Tub67C*^{4}/-. Samples consisted of ^{35}S-methionine-labeled protein from two ovaries plus unlabeled protein from either 30 ovaries or 100 unfertilized eggs. Ovaries were used as a source of labeled protein for both sets of samples because there is no detectable synthesis of αTUB67C in unfertilized eggs. Immunoblots of ovary protein separated on two-dimensional gels and stained with both anti-αTUB67C and a commercial anti-α-tubulin that recognizes all of the *Drosophila* α-tubulins are shown in the top row; autoradiograms from these blots are shown in the second row. Immunoblots of protein from unfertilized eggs (plus labeled ovary protein) are in row 3; autoradiograms of the blots in row 3 are shown in row 4. Small downward-pointing arrowheads indicate the position of αTUB67C. Large upward-pointing arrowheads indicate the primary translation product of αTUB84B/84D; a complex array of increasingly acidic post-translationally modified forms of αTUB84B/84D are also seen in the antibody-stained panels. Small upward-pointing arrowheads indicate the position of a presumptive αTUB67C degradation product that accumulates in unfertilized eggs. Alleles 1, 2, and 3 show detectable accumulation of αTUB67C in ovaries. As is evident by comparing total αTUB84B/84D protein among panels in the top row, the yield of tubulin from ovary samples is highly variable, presumably reflecting variability in the proportion of late-stage egg chambers present in a given sample. Comparison of αTUB67C pool sizes between samples must therefore be made only between the ratios of αTUB67C/αTUB84B+84D.

Table 1. Maternal-effect lethality of α*Tub67C* mutations

	Lethal phase of progeny					
	% Egg/embryo		%	%		
Maternal genotype	W	B	Larva	Pupa	∑	*n*
ri e/Df(3R)AC1	28	5	17	2	52	654
α*Tub67C*^{1}/*Df(3R)AC1*	91	9	0	0	100	618
α*Tub67C*^{2}/*Df(3R)AC1*	100	0	0	0	100	1000
α*Tub67C*^{3}/*Df(3R)AC1*	97.3	2.5	0.2	0	100	600
α*Tub67C*^{4}/*Df(3R)AC1*	100	0	0	0	100	545
ri e/ri e	9		19	1.5	29.5	500
α*Tub67C*^{1}/α*Tub67C*^{1}	100	0	0	0	100	568
α*Tub67C*^{2}/α*Tub67C*^{2}	94.5	1.5	2	0	98	529
α*Tub67C*^{1}/α*Tub67C*^{2}	99.1	0.3	0.2	0	99.6	500
α*Tub67C*^{1}/α*Tub67C*^{4}	99.6	0.2	0.2	0	100	525
α*Tub67C*^{2}/α*Tub67C*^{4}	99.3	0.7	0	0	100	565
α*Tub67C*^{3}/α*Tub67C*^{4}	97.5	100	0	0	100	610

Effective lethal phases are shown for all four hemizygous mutant genotypes, two mutant homozygotes, and several interallelic heterozygotes. W, white undeveloped, eggs; B, brown necrotic embryos; ∑, total % lethality; *n*, sample size.

tions prevent alleles *3* and *4* from being made homozygous. Paternal genotype had no effect on viability (data not shown).

Females of all four hemizygous mutant genotypes produced a large percentage of eggs that appeared to be unfertilized based on color (necrotic embryos discolor, unfertilized eggs remain white). Samples of eggs from these genotypes were stained with an anti-sperm antibody (Karr, 1991) to determined the proportion of eggs that had been inseminated. As shown in Table 2, the frequency of spermless eggs was apparently elevated, compared to the control value, for two of the genotypes, *3/-* and *4/-*, but not for *1/-*

Table 2. Stages of development affected by mutant α*Tub67C* alleles

Maternal genotype	% No sperm	*n*	Stage of development: % 0 NUC	% 1-3 NUC	% PCB	% CB	% G	*n*
ri e/Df(3R)AC1	6.7	74	2.9	1.5	0	0	95.6	68
α*Tub67C*^{1}/*Df(3R)AC1*	5	20	30.9	52.7	16.4	0	0	55
α*Tub67C*^{2}/*Df(3R)AC1*	11.1	81	13	84	3	0	0	69
α*Tub67C*^{3}/*Df(3R)AC1*	21.5	51	40	30.9	7.3	14.5	7.3	55
α*Tub67C*^{4}/*Df(3R)AC1*	21.2	33	44	48.2	1.6	4.7	1.5	64
ri e/ri e			8.6		0	3.7	87.7	81
α*Tub67C*^{1}/α*Tub67C*^{2}			77	21.4	1.6	0	0	61
α*Tub67C*^{1}/α*Tub67C*^{4}			0	0	84.1	15.9	0	44
α*Tub67C*^{2}/α*Tub67C*^{4}			0	0	93.6	6.4	0	62
α*Tub67C*^{3}/α*Tub67C*^{4}			44.7	26.3	29	0	0	38

0-3 hour eggs were assayed for sperm antigens. Nuclei were counted or embryo morphology examined to determine the developmental stage of each animal in samples of 3-10 hour (*1/4* and *3/4*) or 4-7 hour (all remaining genotypes) embryos stained with anti-DNA. No sperm, frequency of eggs with no evidence of sperm antigens; 0 NUC, no stained nuclei were evident; 1-3 NUC, 1, 2, or 3 nuclei were scored; PCB, 4 or more nuclei but pre-cellular blastoderm; CB, at least partial cellularization; G, gastrulation or beyond; *n*, sample size.

and *2/-*. α*Tub67C* mutations may affect micropyle morphology or otherwise interfere with successful sperm entry, or degenerative processes may be occurring in some oocytes that prevent sperm entry or lead to rapid decay of the sperm tail once inside the egg. Nevertheless, close to 80% of the unhatched eggs produced by mutant females had been inseminated.

A more precise stage of developmental arrest was determined for eggs from most of the genotypes included in Table 1 by examining eggs 4-7 hours post-egg-lay (except *1/4* and *3/4* samples, which were 3-10 hours old) stained with anti-DNA. Results are shown in Table 2. In the control sample almost all of the eggs had completed cleavage and cellularization and had begun or completed gastrulation, while embryos that had reached gastrulation were rare among the mutant genotypes. None of the eggs from *1/-* or *2/-* mothers had reached cellular blastoderm, and most of the *3/-* and *4/-* animals that did achieve cellularization or gastrulation were highly aberrant, showing uneven nuclear distribution, low nuclear density at the cortex, and incomplete cellularization.

The large majority of eggs from these four mutant genotypes had approximately 3 or fewer nuclei, ranging from 71% for allele *3* to 92% for allele *4*, and most of these nuclei were polyploid. The nuclear count is approximate because the aberrant morphology of these nuclei was sometimes confounding. In many cases multiple sets of chromosomes were tightly clustered and clearly belonged to a single nucleus, but in other cases chromosomes were dispersed in ambiguous patterns. As shown in Table 2, many of the mutant genotypes produced a high frequency of eggs in which no stained nuclei were detected. Among *1/-*, *2/-*, *3/-*, *4/-*, *1/2*, and *3/4* eggs, the nullo-nuclei class accounts for 22-45% of the eggs scored, yet *ri e/-*, *1/4*, and *2/4* samples had few or no eggs in this class. These two groups of genotypes formed by the frequency of nullo-nuclei eggs are also defined by the frequency of eggs that enter cleavage - low and high, respectively. We think it likely that eggs with no evident nuclei are a subset of oocytes that fail to enter cleavage in which the chromosomes have decondensed and are not visible with our staining methods. The subset might simply be the older eggs within the sample, or it might reflect some physiological difference among mutant oocytes. Alternatively, the nullo class of oocytes may be composed of necrotic eggs in which nuclei fail to stain due to degradative processes. If these eggs are necrotic, it might be more appropriate to view the nullo class as a measure of oogenic failure per se rather than as mature oocytes incapable of progressing to embryogenesis.

Despite this uncertainty about the origin of the nullo oocytes, it is clear that all four mutant α*Tub67C* alleles block or disrupt developmental events that normally follow insemination of the egg. The proportion of embryos with less than four nuclei at least 3 hours post-egg-lay is high for all four hemizygous genotypes, ranging from 71% to 97%. Females hemizygous for alleles *3* and *4* produced a few eggs that developed beyond cellular blastoderm, but animals completing embryogenesis were extremely rare. Allele *2* produced the most severe phenotype in terms of embryonic development, with only 3% of eggs from *2/-* females undergoing even aberrant cleavage. A larger proportion of eggs from *1/-* females initiated cleavage, but the majority had three or fewer nuclei. Cellularization was never observed in embryos from *1/-* or *2/-* females. Although allele *2* is the strongest of the four mutant alleles by these criteria, it is not a functional null. As shown in Table 1, females homozygous for α*Tub67C*^{2} produce eggs with improved viability compared to *2*/-females. Alleles *3* and *4* share the basic phenotypic characteristics of allele *2*, but a progressively larger fraction of eggs from *4/-* and *3/-* females, respectively, initiate cleavage. Almost 15% of eggs from *3/-* females achieve at least partial cellularization. More than half the eggs from *1/-* females entered cleavage, but even partially cellularized embryos were never observed in this group. Based on the average degree of development achieved by eggs of the hemizygous mutant genotypes shown in Table 2, the four α*Tub67C* alleles can be ranked from most severe to least severe as follows: *2* < *4* < *1* < *3*.

Comparing developmental potential of eggs from the four interallelic genotypes for which we have data with that of eggs from each combination's relevant hemizygotes, e.g., *1/2* compared to *1/-* and *2/-*, shows that *1/2* and *3/4* behave as expected based on simple additive effects, but *2/4* and

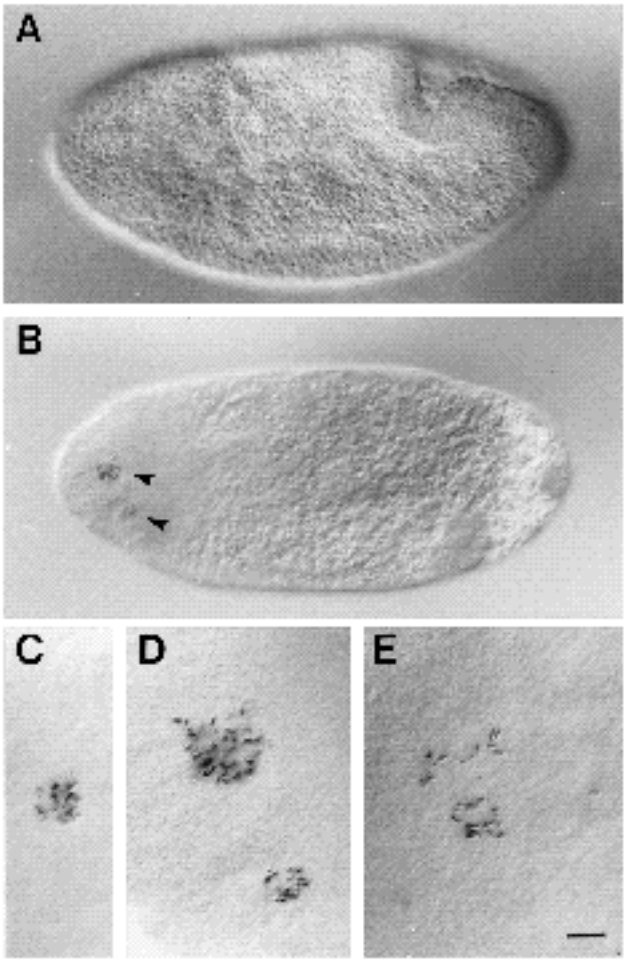

Fig. 2. Early arrest phenotype of α*Tub67C* mutations. Nuclei of 4-7 hour old eggs/embryos are stained with anti-DNA. (A) Stage 6 embryo derived from a *Df(3L)AC1/ri e* female. Nuclei are visible as small, dense dots of stain distributed relatively uniformly across the surface of the gastrulating embryo. (B) Undeveloped oocyte from an $\alpha Tub67C^{2}/Df(3L)AC1$ female showing a typical binucleate phenotype; the two nuclei indicated with arrow heads are shown at higher magnification in D. Additional chromosomes lie out of the plane of focus. (C) Polyploid nucleus from a mononucleate oocyte. (E) Ambiguous chromosome array that may reflect aborted meiosis. Anterior is to the left, dorsal to the top, in A and B. Bar ≈ 26 μm for A and B, 8.3 μm for C-E.

1/4 do not. For both of the latter, females of the interallelic genotype produced eggs with greater average developmental potential than either hemizygote, suggesting that the products of these allele pairs interact to produce somewhat better microtubule function than either mutant protein alone. In both cases, the improved function supports meiosis and some of the cleavage divisions, but is not sufficient to support embryonic development into the gastrulation stage.

Examples of the early arrest phenotype associated with all four α*Tub67C* mutations are shown in Fig. 2. Mono- and binucleate arrangements were the most common phenotype (Fig. 2B,D). Eggs in this class have a polyploid nucleus in the anterior quarter of the egg at a variable position along the dorsal-ventral axis. We estimate chromosome number in these large nuclei to range from 3N to 8N. Second nuclei most often lie within 50 μm of the first, but not immediately adjacent as would be expected of recent meiotic products, and in some cases are more than 150 μm away. Chromosome numbers in second nuclei range from approximately haploid to tetraploid. Third nuclei, when present, are typically within 25 μm of one of the other two with a chromosome number in the haploid to diploid range, although a few single chromosomes were observed. Nuclei are usually surrounded by yolk-free cytoplasm, as the female pronucleus is in normal embryos, but these cytoplasmic regions are large and are not always associated with a detectable nucleus. Yolk-free cytoplasm exists as both discreet islands (not shown) and irregularly shaped masses extending from the egg periphery (Fig. 2B).

Examples of mutant embryos capable of supporting some mitotic activity are shown in Fig. 3. The embryo in Fig. 3C illustrates the high end of the phenotypic range for the more severe alleles. The number and synchronicity of nuclei place this embryo at stage 4, having undergone 9 cleavage divisions, despite its age of at least 4 hours (stage 4 in a wild-type embryo ends at about 2 hours 10 minutes post-oviposition; Campos-Ortega and Hartenstein, 1985). In addition to the delayed developmental time, distribution of nuclei at the cortex is irregular in some regions. The embryos shown in Fig. 3D-F qualify as blastoderm stage in that nuclei are present at the cortex, but the blastoderm is extremely aberrant. The embryo in Fig. 3E consists of what appear to be 20-30 highly polyploid giant nuclei. The embryos in Fig. 3D,F have some giant nuclei, but also many of approximately normal size. The distribution of these nuclei at the cortex is irregular, producing clumps and voids, nuclear cycles are asynchronous, and the distribution of yolk is uneven. The overall phenotype suggests a post-cellular blastoderm embryo, yet no evidence of cellularization was observed.

The simplest interpretation of these observations is that the ability to accomplish nuclear division, either meiotic or mitotic, is compromised in oocytes lacking wild-type α*Tub67C* protein. The nucleus of a mature *Drosophila* oocyte is arrested at metaphase of meiosis I (Mahowald and Kambysellis, 1980). The completion of meiosis is triggered by activation of the egg, normally achieved by insemination or ovulation (Doane, 1960; Mahowald et al., 1983). One of the meiotic products functions as the female pronucleus; two or all three of the remaining polar nuclei often fuse to form diploid or triploid polar bodies. [Note: Campos-Ortega and Hartenstein (1985) attributed the rarity of fertilized eggs with three haploid polar nuclei to the routine absence of meiosis II in one of the products of meiosis I, while Doane (1960) attributed a similar observation in uninseminated eggs to the fusion of polar bodies subsequent to the completion of meiosis. Using high resolution techniques to examine meiosis in both inseminated and uninseminated eggs, William Theurkauf (Department of Biochemistry and Cell Biology, State University of New York, Stony Brook, NY 11794-0001, USA) has shown that meiosis is indeed complete in oocyte nuclei, whether inseminated or not, and is typically followed by fusion of two or more polar nuclei (personal communication).] Among the eggs from α*Tub67C* hemizygous mutant females described

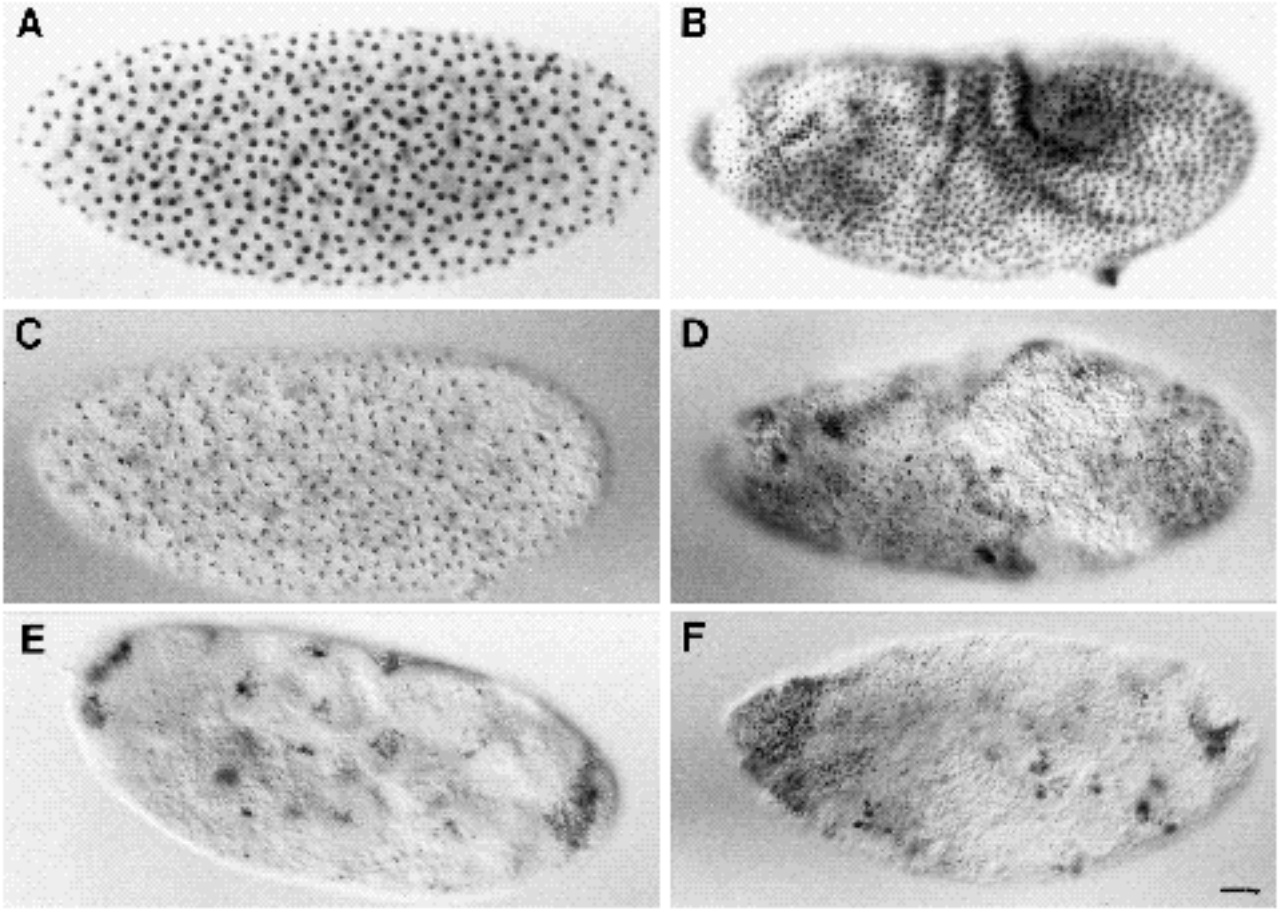

Fig. 3. Embryonic phenotypes of α*Tub67C* mutations. Nuclei of 4-7 hour old embryos are stained with anti-DNA. (A) Embryo from a *w* female that has reached syncytial blastoderm. (B) Gastrulating embryo (stage 8) from a *w* female. (C) An atypical embryo from a α*Tub67C*^{4}/- female that has formed a relatively normal syncytial blastoderm. Development is either delayed or arrested (a comparable wild-type embryo would be less than 90 minutes old; this animal is at least 4 hours old) and regions of the posterodorsal cortex are devoid of nuclei. (D,F) Blastoderm embryos from α*Tub67C*^{3}/- females. Nuclei range from apparently diploid or less, to highly polyploid, and their distribution is extremely nonuniform. Distribution of yolk is also irregular, seen most clearly in D as a large mass reaching to the cortex between about 20% and 50% egg length. No cellularization was detected in these embryos. (E) Embryo from an α*Tub67C*^{2}/α*Tub67C*^{4} female. Extremely polyploid nuclei surrounded by giant cytoplasmic islands are evident in this embryo. In all panels, anterior is to the left, dorsal to the top. Bar ≈ 26 μm.

in Table 2, if only oocytes in which at least one nucleus was stained are considered, all but the weakest allele produced a majority of eggs with either one or two nuclei - 76%, 83%, and 69% for alleles *1*, *2*, and *4*, respectively.

We interpret the nuclear configuration of binucleate eggs as an unreduced oocyte nucleus and a male pronucleus, one or both of which may have undergone an additional one or two rounds of DNA replication. The mononucleate eggs could be either uninseminated eggs that failed to complete meiosis upon activation by ovulation or inseminated eggs in which the male pronucleus fused with the unreduced oocyte nucleus. Presumably the trinucleate eggs are the result of partially successful meiosis while the later arrest phenotype identifies embryos that completed meiosis and proceeded with cleavage, with varying degrees of success.

We are not able to determine from these data whether nuclear migration is affected by mutations in α*Tub67C*. Nuclei do migrate to the cortex in mutant animals, but significant numbers of nuclei are present only in less severely affected embryos. Therefore, we cannot eliminate the possibility that αTUB67C is required for nuclear migration, but when αTUB67C function is sufficient to produce cleavage nuclei it is also sufficient to support nuclear migration.

Microtubule arrays in α*Tub67C* mutant oocytes and embryos

It is clear from the developmental analysis of oocytes having only mutant αTUB67C that spindle function is compromised in these genotypes. Eggs from hemizygous mutant females were stained with either anti-αTUB67C or anti-αTUB84B/84D to identify microtubule-containing structures in these mutant oocytes and embryos. In wild-type embryos these two antibodies produce identical staining patterns. Essentially no staining pattern was observed in eggs from *2*/- and *4*/- females stained for αTUB67C; the faint ooplasmic staining could not be distinguished from background (not shown). Examples of oocytes/embryos stained for αTUB84B/84D are shown in Fig. 4. Young

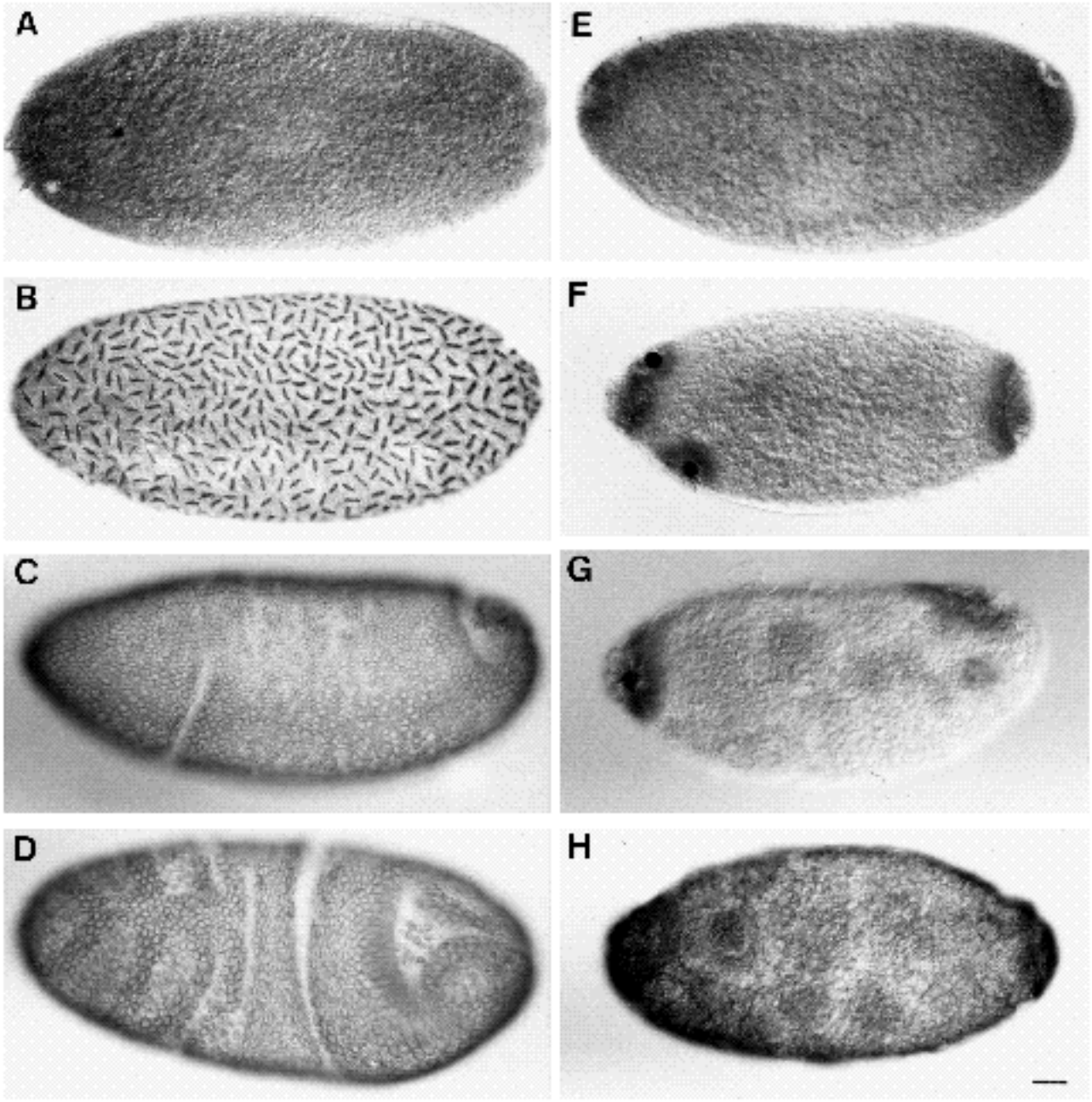

Fig. 4. Distribution of tubulin in α*Tub67C* mutations. Embryos are stained with anti-αTUB84B/84D. (A-D) Control oocyte/embryos 0-4 hours old showing tubulin staining patterns at different stages of development. (A) Cytoplasmic microtubules in an oocyte (probably an unfertilized egg). The dense plaque of tubulin at about 80% egg length probably marks a polar body; the void at the anteroventral cortex is an artifact. (B) Spindles in a syncytial blastoderm embryo. (C,D) Cytoplasmic microtubules in gastrulating embryos. (E-H) Cytoplasmic tubulin in $\alpha TUB67C^{4}$ (E-G) or $\alpha TUB67C^{2}$ (H), 0-4 hour old (E,H) or 0-7 hour old (F,G) oocytes/embryos. Tubulin distribution is nonuniform, typically with higher concentrations at the poles (E-H) and in large cytoplasmic islands (F-H). Extremely dense tubulin plaques encase polyploid nuclei (F, G). In all panels, anterior is to the left, dorsal to the top. Bar ≈ 26 μm.

eggs/embryos (no more than 3 hours old) from *2*/- and *4*/- females stained for αTUB84B/84D had the same uniform staining at the cortical surface as seen in undeveloped eggs from control females (Fig. 4A). The dense plaque of tubulin seen at about 80% egg-length in the oocyte shown in Fig. 4A presumably corresponds to a polar body. Similar extremely dense tubulin plaques in mutant embryos, such as those in Fig. 4F,G, were seen to colocalize with DNA when embryos were double stained with anti-αTUB84B/84D and the fluorescent DNA stain, DAPI (data not shown). The numbers and locations of these tubulin plaques in mutant embryos suggest that they correspond to polyploid nuclei such as those shown in Fig. 2B-E.

Among samples that include older animals (0-5 and 0-7 hour collections), the microtubule network in some mutant oocytes/embryos appears more fibrous and the distribution

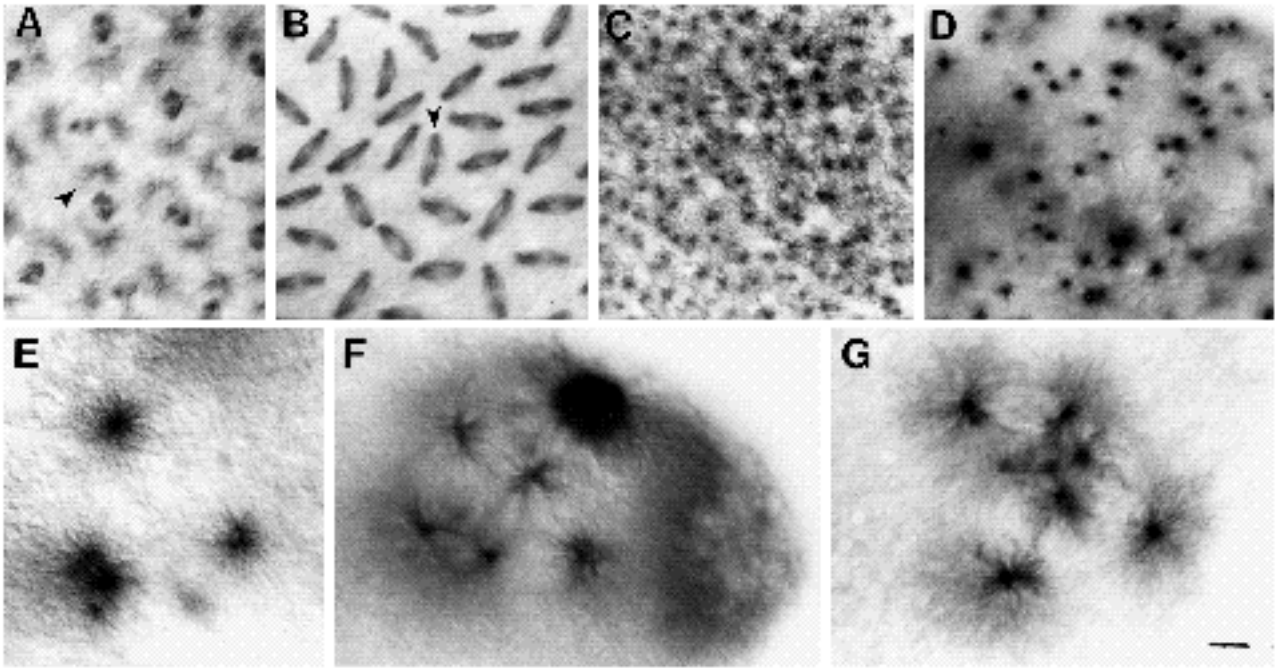

Fig. 5. Asters and aster-like structures in αTUB67C^{2} and αTUB67C^{4} embryos. Embryos were stained with anti-αTub84B/84D. (A,B) Spindles in embryos with wild-type αTUB67C. Arrowheads indicate asters in metaphase/anaphase (B) and telophase (A) mitotic spindles. (C-G) Asters and aster-like structures in mutant embryos. (C,D) Fields of asters, some with extremely dense cores, in αTUB67C^{2} embryos. (E-G) Huge aster-like structures that form in aging αTUB67C^{4} embryos. Bar ≈ 8.3 μm for all panels.

of microtubules is nonuniform. Regions of more intense staining are typically seen at both poles (Fig. 4E-H), and islands of more densely packed microtubules form in some individuals (Fig. 4G,H). Posterior constrictions are common in mutant animals, producing a peculiar muffin-like protrusion at the posterior pole (Fig. 4F,H). Anterior deformations are observed as well, but they are less stereotypical. Spindle structures observed in these mutants were limited to aster-like formations, shown in Fig. 5. A few mutant individuals had large numbers of centrosomes at the cortex projecting microtubule arrays of varying lengths (Fig. 5C,D). Aster-like structures of extremely large size (Fig. 5E-G) were also observed among oocytes from both mutant genotypes, but only among individuals from the longest collection time (0-7 hours), indicating that the formation of these aberrant structures is age-dependent. Spindles of more normal appearance must form in a few *2*/-and *4*/- eggs, since a few oocytes can support nuclear division (see Fig. 3C), but none were observed among these samples.

In contrast, recognizable mitotic spindles form in eggs produced by *1*/- and *3*/- females. For *3*/- females, spindles were observed only when embryos were stained with anti-αTUB84B/84D. Both anti-αTUB67C and anti-αTUB84B/84D stain *1*/- spindles. The range of spindle morphology observed in these samples, often within the same egg, is illustrated in Fig. 6. In addition to spindles with the relatively thin, pointed shape typical of *Drosophila*, some in the normal configuration and some bent into a canoe shape, large ovoid spindles, slender needle-shaped spindles, multipolar spindles, half spindles and fused spindle masses were observed (Fig. 6B-I). The large spindles are approximately twice the width of normal spindles, with little or no change in length, and primarily appear to have extra kinetochore microtubules. Although only tubulin staining is shown, the DNA content of the spindle in Fig. 6B was viewed using DAPI staining; chromosomes were perfectly aligned along the metaphase plate, with DNA content appearing to fall somewhere between 6N and 8N. Slender spindles are about half the normal width, shorter by variable amounts, and seem to be composed of only interpolar microtubules. Assorted fragments are also present, including isolated asters and small bundles of parallel microtubules with no constriction at the poles. Under-sized spindles were occasionally observed in *w* controls, but over-sized spindles were never observed among control animals.

Dosage effects of wild-type αTUB67C

The results of our mutational analysis of α*Tub67C* indicate that αTUB67C is required for oocyte meiosis and early embryogenesis. The rescue of these mutations by transgenic copies of α*Tub67C*, but not α*Tub84B*, demonstrates a qualitative requirement for αTUB67C. Thus, a lower limit exits on the ratio of αTUB67C/αTUB84B+84D that will support normal development. There is also an upper limit on this ratio.

In the process of constructing and maintaining transgenic α*Tub67C* lines it became evident that some of these genotypes had significantly reduced female fertility. The transgenic line used for complementation in previous experiments, *w; P{w*$^{+}$ *αTub67C*$^{+}$*}1/SM5*, which appears to carry a single insert based on intensity of eye color, fully complements α*Tub67C* mutations without itself having large

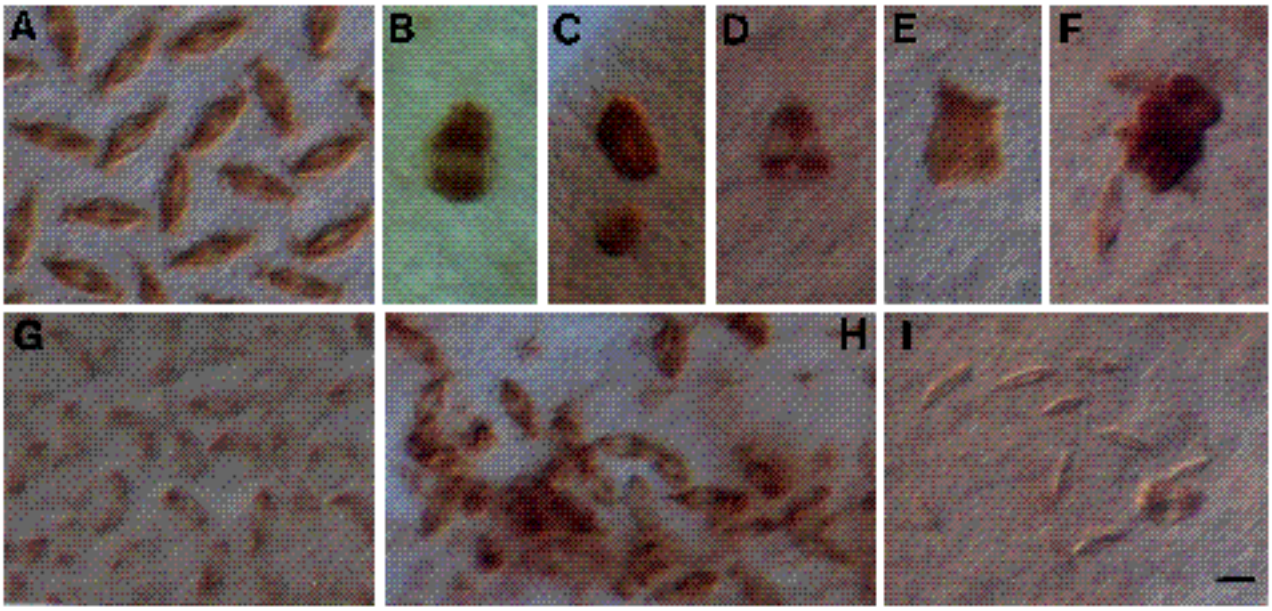

Fig. 6. Aberrant spindles in αTUB67C[1] and αTUB67C[3] embryos. Mutant embryos were stained with anti-αTub84B/84D. (A) Wild-type metaphase/anaphase spindles stained with anti-αTUB67C. (B,F,I) αTUB67C[3] embryos. (C-E,G,H) αTUB67C[1] embryos. (B) Barrel-shaped spindle. (C) Rectangular and half-spindle. (D) Tripolar spindle. (E) Multipolar spindle. (F) Fused spindle mass. (G) Field of spindles including both normal and canoe-shaped spindles. (H) Field of spindles, many fused pole to pole. (I) One barrel-shaped spindle with abundant kinetochore microtubules and a group of needle-shaped spindles composed of only interpolar microtubules. Bar ≈ 5 μm.

Table 3. Maternal-effect lethality resulting from increased dosage of α*Tub67C*

Genotype	% E	% L	% P	∑	*n*
α*Tub67C*$^{+}$*-4*	88.4	5.4	0.6	94.4	500
w	12.8	10	2.6	25.4	500

Percent lethality through development is shown for progeny of 2-5 day old females. E, embryo; L, larva; P, pupa; *n*, sample size; α*Tub67C*$^{+}$*-4, w; TM3, P{w*$^{+}$ α*Tub67C*$^{+}$*}4/+*.

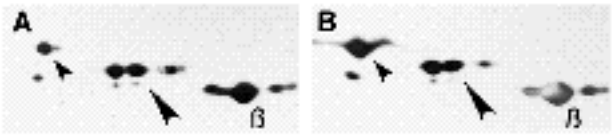

Fig. 7. Excess αTUB67C accumulates in multicopy α*Tub67C* females. Immunoblots of tubulin proteins from unfertilized eggs derived from Oregon-R (A) or *P{w*$^{+}$ α*Tub67C*$^{+}$*}4, TM3/+* (B) females. Small arrowheads indicate αTUB67C, large arrowheads point to the group of αTUB84B/84D proteins. β-tubulins are at the lower right in each panel.

effects on female fertility. However, another transgenic line, *w; +/TM3, P{w*$^{+}$, α*Tub67C*$^{+}$*}4* (α*Tub67C*$^{+}$*-4* for short), which appears to carry two inserts judging from eye color, has a very strong maternal effect on embryonic viability. As shown in Table 3, less than 6% of embryos from α*Tub67C*$^{+}$*-4* females produced viable adults. Intermediate levels of female sterility were observed in other transgenic lines.

The effect of the transgenes on female fertility is a bona fide dosage-effect of α*Tub67C*. Immunoblots of tubulin protein from unfertilized eggs produced by wild-type and α*Tub67C*$^{+}$*-4* females, shown in Fig. 7, demonstrate an increase in accumulation of αTUB67C in oocytes from transgenic mothers. The ratio of αTUB67C/αTUB84B+84D in eggs from α*Tub67C*$^{+}$*-4* females is roughly 1:1, compared to approximately 1:4 in eggs from wild-type females.

The sterility of α*Tub67C*$^{+}$*-4* females can be at least partially reversed by simultaneously increasing the dose of α*Tub84B*. A single copy of *P{w*$^{+}$ α*Tub84B*$^{+}$*}4*, the transgene that had no effect on the phenotypes of α*Tub67C* mutations, increases fertility of α*Tub67C*$^{+}$*-4* females to 56% (*n*=500). Taken together, these results demonstrate that the ratio of αTUB67C/αTUB84B+84D must fall within certain limits for the maternally supplied α-tubulin pool to support normal development.

Phenotypic effects of excess αTUB67C

In contrast to loss-of-function mutations in α*Tub67C*, overproduction of the αTUB67C isotype appears to have little or no effect on meiosis. Essentially all of the eggs from α*Tub67C*$^{+}$*-4* females enter cleavage and the majority gastrulate, although most of these animals are highly aberrant. Evidence of dysfunctional mitotic spindles in these females is provided by embryos stained for DNA, shown in Fig. 8B,C. Both hypoploid and grossly hyperploid nuclei are present, synchronicity of the nuclear cycles during cleavage is disrupted, and the cortex is unevenly populated with nuclei in blastoderm stages.

The bizarre morphology of spindles formed in these embryos, revealed by staining with any of the anti-tubulin antibodies, is shown in Figs 8E,F, 9. The spindles themselves are characterized by a highly diverse range of shapes

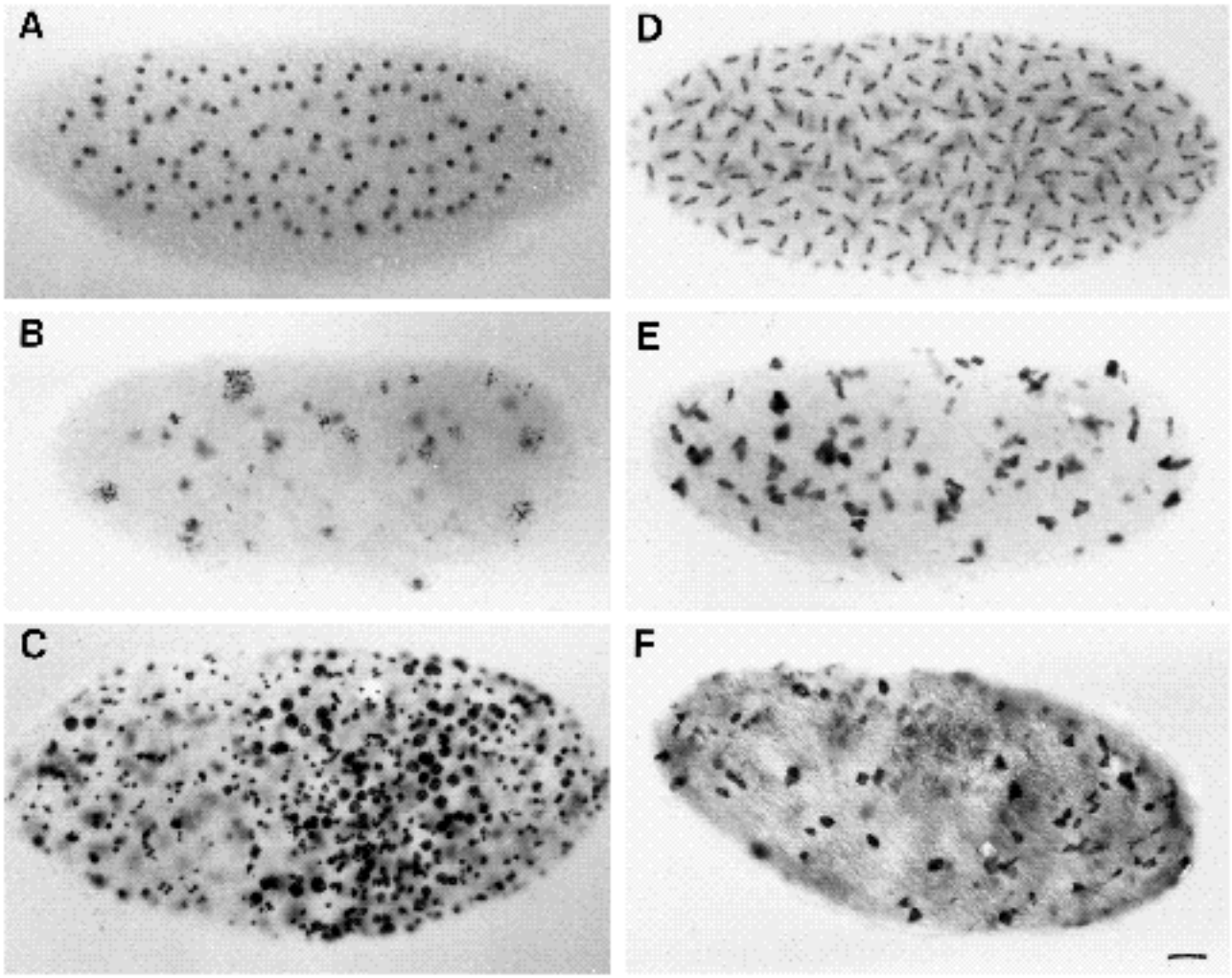

Fig. 8. Excess αTUB67C disrupts cleavage. Embryos A-C were stained with anti-DNA, D,E were stained with anti-αTUB67C, F was stained with anti-αTUB84B/84D. (A,D) Embryos from wild-type females showing cleavage nuclei and spindles. (B,C,E,F) Embryos from *P{w*$^{+}$ *αTub67C*$^{+}$*}4, TM3/+* females. Spindles form and function to some extent, but many nuclei are polyploid (B,C) and spindles are often large and misshapen (E,F). Bar ≈ 26 μm.

and sizes. Although *αTub67C*$^{+}$*-4* spindles are, on average, larger and much denser than wild-type spindles, and often multipolar, some small and many monopolar spindles are also observed. The failure to form boundaries defining individual spindles is also a frequent occurrence among spindles with excess αTUB67C. Spindle fusions in all orientations - pole to pole, pole to midbody, midbody to midbody - are typical in these embryos. In addition, networks of asters and small microtubule bundles fill much of the space between spindles in many embryos, illustrated in Figs 8F, 9C. This microtubule network stains more intensely with either anti-αTUB84B/84D or anti-α-tubulin than with anti-αTUB67C. The clear background seen in Fig. 8E compared to 8F is typical and can be accounted for by an enrichment of αTUB84B/84D in these primarily astral fields. This is the only example of differential isotype concentrations we observed.

Dominant phenotypes of α*Tub67C* mutations

We have focused on the recessive phenotypes of *αTub67C* mutations, but all four alleles also show a dominant reduction in female fertility. As shown in Table 4, heterozygous mutant females produced 17%-49% fewer viable embryos than did control females, with allele *3* having the strongest dominant effect. A large reduction in egg viability was also observed for *Df(3L)AC1*.

On average, inviable oocytes from heterozygous mutant females develop further than those from hemizygous mutant females. In these samples 25% (*4/TM3*)-53% (*3/TM3*) of the eggs that failed to hatch were necrotic, compared to 0% for these alleles as hemizygotes (see Table 1). However, for allele *4* at least, fertilized but undeveloped oocytes are also common. The 140 unhatched eggs from the *4/TM3* sample described in Table 4 were stained for sperm tails. 70 of the 86 eggs that survived the fixation and staining process intact contained sperm tail antigen, and 40 of these showed no signs of development. Thus, if this sample is representative (we have no reason to suspect preferential loss of any given class of egg from the fixation and staining process but it remains a possibility),

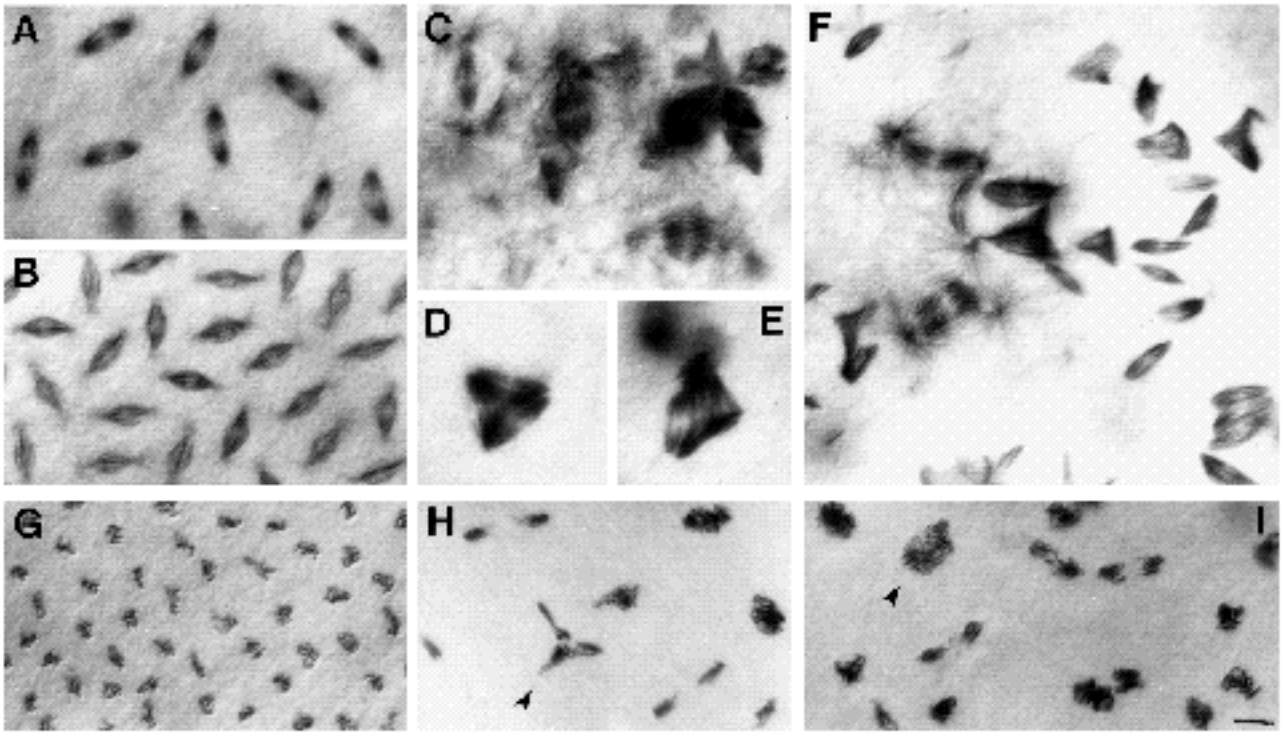

Fig. 9. Aberrant spindle morphology and function in the presence of excess αTUB67C. Embryos in A,B,D,E were stained with anti-αTUB67C. C,F were stained with anti-β-tubulin. G-I were stained with anti-DNA. (A,B) Wild-type cleavage spindles. (C-F) Spindles formed in embryos from *P{w⁺ αTub67C⁺}4, TM3*/+ females. (C) Large and/or multi-aster spindles. (D) Tripolar spindle. (E) Multipolar spindle. (F) Undersized, multipolar, and fused spindles, some with large asters, some with none. (G) Cleavage nuclei of wild-type embryo. (H,I) Normal and aberrant cleavage nuclei. A wide range of ploidy can be seen among nuclei in close proximity. Arrowhead in H indicates a tripolar figure. Arrowhead in I indicates a highly polyploid nucleus. Bar ≈ 7 μm for all panels.

approximately 19% of the unhatched eggs had not been penetrated by sperm, about 46% were inseminated but failed to develop, and approximately 35% arrested during embryonic cleavage.

The effects of an additional dose of wild-type α*Tub67C* on the semidominant female sterility of α*Tub67C*^{3} and *Df(3L)AC1* are shown in Table 4. The additional wild-type copy of α*Tub67C* provided by the transgene restored egg hatchability to control levels for α*Tub67C*^{3}. A transgenic copy of α*Tub67C* also improved fertility of *Df(3L)AC1* by approximately 38% (full restoration of *Df(3L)AC1* fertility is not expected since *M(3)67C* is not covered by the transgene). An additional copy of α*Tub84B* had no effect on fertility of either α*Tub67C*^{3} or *Df(3L)AC1* heterozygotes, as shown in Table 4. These data demonstrate that α*Tub67C* is a haplo-insufficient locus.

Recall that the rank of the four α*Tub67C* alleles based on their recessive phenotypes is *2 < 4 < 1 < 3*. However, if based on the semidominant phenotypes, the rank is *3 < 1 = 2 = 4*, despite the fact that both dominant and recessive components of the mutant phenotype reflect loss of α*Tub67C* function. One possible explanation for the divergent rank of allele *3* is that an allele-specific interaction between αTUB67C^3 and wild-type protein accounts for the increased severity of this allele's dominant phenotype. Typically such an allele would behave as an antimorph and the addition of a single wild-type gene would not restore the wild-type phenotype. However, the instability of αTUB67C^3 results in a ratio of *3* :+ protein that is significantly below 1:1 (see Fig. 1, row three of the column labled 3), which might allow antimorphic effects of αTUB67C^3 to be completely overcome by a single additional dose of wild-type α*Tub67C*.

Table 4. α*Tub67C* alleles are semidominant

Genotype	% Viable embryos	% White eggs	% Necrotic embryos	*n*
ri e/TM3	92	3	5	625
α*Tub67C*^{1}/*TM3*	75	12	13	525
α*Tub67C*^{2}/*TM3*	76	16	8	464
α*Tub67C*^{3}/*TM3*	47	25	28	500
α*Tub67C*^{4}/*TM3*	72	21	7	500
w; α*Tub67C*$^+$*-1*/+; α*Tub67C*^{3}/*TM3*	90	4	6	497
w; α*Tub67C*^{3}/*TM3*	56	29	15	554
w; α*Tub84B*$^+$*-4*/+; α*Tub67C*^{3}/*TM3*	61	15	24	520
SM5/+; *Df(3L)AC1*/+	56	27	17	504
α*Tub67C*$^+$*-1*/+; *Df(3L)AC1*/+	77	11	12	500
α*Tub84B*$^+$*-4*/+; *Df(3L)AC1*/+	53	35	12	507

The fraction of viable embryos produced by females of the genotypes shown was used as a measure of dominance. The proportion of inviable eggs that remained white 30 hours or more post-collection, and thus were either unfertilized eggs or early-arrest oocytes/embryos, and the proportion that proceeded far enough into embryogenesis to contain necrotic tissue, are also shown. α*Tub67C*$^+$*-1 = P{w*$^+$ α*Tub67C*$^+$*}1*; α*Tub84B*$^+$*-4 = P{w*$^+$ α*Tub84B*$^+$*}4*.

Oogenesis in α*Tub67C* mutations

The effects α*Tub67C* mutations on premeiotic stages of oogenesis have not been well characterized. However, since some of these observations may prove useful for further analyses, a brief summary follows.

Casual observation of egg morphology suggested that hemizygous mutant females produced more short or flaccid eggs than control females. A few samples were scored for abnormal morphological characteristics: absent, short, or otherwise misshapen chorionic appendages were found in 12% of *2/4*-derived eggs (*n*=165), while no abnormal filaments were observed among eggs from *1/2* (*n*=300), *1/4* (*n*=524), *3/4* (*n*=200), or control females.

Distribution of α-tubulin in developing oocytes, and their general morphology, was examined in hemizygous mutant ovaries stained with anti-αTUB67C, anti-αTUB84B/84D, or the DNA stain feulgen. Normal isotype distribution patterns were observed in all four genotypes: both classes of α-tubulin were detected in egg chambers beginning at stage 2, both were found in nurse cells and oocytes in later stage egg chambers, and only αTUB84B/84D was detected in follicle cells. Detection of αTUB67C antigen in oocytes from *4/-* females when none was detected on immunoblots (see Fig. 1) presumably reflects the increased sensitivity of whole-tissue staining. A few necrotic egg chambers were observed. In feulgen stained material, a variety of abnormalities were observed in a minority of follicles. The most common defects were ventral displacement of the oocyte nucleus from its characteristic dorsal position, abnormal follicle cell movements, and aberrant ratios of oocyte to nurse cell volumes.

The relatively subtle effects of α*Tub67C* mutations on developing egg chambers may reflect a genuinely limited role for this tubulin during the growth stages of oogenesis. However, none of the mutations tested here are protein nulls. We cannot exclude the possibility that in these mutant genotypes an effectively larger pool of αTUB67C is available to developing follicles than to mature oocytes, either by increased stability of the mutant proteins themselves or the presence of other components, such as MAPs, that enhance the function of the mutant tubulin.

DISCUSSION

The results presented here demonstrate that the isotypic makeup of the α-tubulin pool of *Drosophila* oocytes and early embryos is critical for both meiotic and mitotic spindle function in this cell. α-tubulins from three genes encoding two isotypic classes of proteins, αTUB84B/84D and αTUB67C, are present in the oocyte. Strong hypomorphic maternal-effect-lethal mutations in α*Tub67C* block meiosis in a majority of affected oocytes, while cleavage mitoses are disrupted in embryos that escape the meiotic block. Increasing the ratio of wild-type αTUB67C in the oocyte is almost as lethal as decreasing it, but only mitotic spindles are adversely affected by excess αTUB67C. The ratio of isotypes appears to be the critical factor, as a simultaneous increase in the dose of α*Tub84B* suppresses the embryonic lethality caused by increasing the dose of α*Tub67C*.

This requirement for αTUB67C is specific to spindles of the oocyte and embryo. Most dividing cells in larvae and pupae contain only αTUB84B and/or αTUB84D, and αTUB84B is the only α-tubulin isotype present in the germ line of adult males (Matthews et al., 1989, 1990). Thus, the generic form of α-tubulin is sufficient to support spindle function in both male meiosis and post-embryonic mitosis, but not in female meiosis or cleavage. The meiotic spindle of oocytes appears to be structurally unusual in several respects (Theurkauf and Hawley, 1992), the most striking feature in the current context being the absence of centrosomes (Sonnenblick, 1950; Theurkauf et al., 1992). Centrosomes, which serve as microtubule organizing centers in most animal cells, are present in both spermatocyte meiotic spindles (Cooper, 1950; Tates, 1971) and mitotic spindles in *Drosophila* (see Glover, 1989). Although speculative at present, we find it an extremely interesting possibility that αTUB67C serves to facilitate the nucleation of microtubules in the absence of centrosomes.

Another interesting aspect of the α*Tub67C* gene has been the possibility that structural properties of this highly diverged isotype allow the unusually rapid assembly and disassembly of *Drosophila* cleavage spindles (Rabinowitz, 1941; Sonnenblick, 1950; Zalokar and Erk, 1976; Foe and Alberts, 1983). αTUB67C is required for normal mitotic spindle function during cleavage, and too much of this isotype poisons spindle activity. An enhanced ability of αTUB67C-containing tubulin pools to initiate microtubule polymerization could account for the loss of spindle function when the ratio of αTUB67C to αTUB84B/84D in these mixed isotype pools exceeds certain limits in either direction. Below some isotype ratio threshold spindle assembly may not be rapid enough, and above some threshold, spindle assembly might be uncontrolled. The density of microtubules in hypermorphic αTUB67C embryos, both within and between spindles, might reflect excessive nucleation of microtubules driven by over-representation of αTUB67C in the tubulin pool.

Although we think it likely that some of the aberrant spindle morphologies observed here are immediate consequences of the isotypic makeup of the tubulin pool, it is equally likely that some are not. In particular, at least some aspects of large size, multipolarity, and spindle fusions, the morphological peculiarities that are shared by hypomorphic and hypermorphic spindles, may be secondary effects of previous spindle dysfunction. Chromosome content and nuclear distribution are probably important factors in determining mitotic spindle morphology. Ploidy is extremely variable in these embryos, ranging from single chromosomes to highly polyploid nuclei, and nuclear spacing is often poor. Some increase in spindle size may reflect a relatively normal response of the mitotic apparatus to the presence of a much larger than normal chromosome complement. Similarly, small spindles and spindle fragments may organize around hypoploid nuclei, individual chromosomes, or chromosome fragments (Church, 1986; Theurkauf and Hawley, 1992). Multipolar and fused spindles might reflect an increased ratio of centrosomes to nuclei resulting from previously failed mitoses (centrosomal division is independent of nuclear division; Freeman et al., 1986), or insufficient space between nuclei. Examination of the first few

cleavage divisions in mutant embryos should reveal whether these gross defects in spindle morphology are a primary attribute of altered isotype pools or the legacy of previously failed mitoses.

Mutant phenotypes associated with both insufficient and excess αTUB67C show variable expressivity. Although the maternal effect lethality of all four loss-of-function mutations is absolute, and the majority of oocytes fail to complete meiosis or arrest very early in embryogenesis, a few animals are able to support more normal spindle function. Similarly, most embryos with excess αTUB67C fail to complete embryogenesis, but a few develop into apparently normal adults. Within individual embryos from both classes of mutation, normal and aberrant spindles can often be seen in close proximity. One component of the variability among individuals may be random differences in maternal loading of individual oocytes. At wild-type tubulin levels, small differences in isotype ratios are probably inconsequential, but in the highly sensitized backgrounds these mutant genotypes represent, even small variations in the maternal contribution might have significant effects on microtubule function. Although other explanations are possible, it seems most likely to us that intracellular variation results from random differences in isotype utilization by a developing spindle. If isotype ratios are most critical at only one or two points during the mitotic cycle, sampling error alone could produce dramatic differences in outcome among individual spindles.

The accumulation of a large excess of αTUB67C tubulin from a small number of extra genes was unexpected, based on extrapolation from tubulin autoregulatory mechanisms found in a wide variety of cultured animal cells (reviewed by Cleveland, 1989). In these cells, an increase or decrease in the pool of unassembled tubulin subunits results in a rapid decrease or increase, respectively, in tubulin synthesis (Ben-Ze'ev et al., 1979; Cleveland et al., 1981; Cleveland, 1989). For β-tubulin at least, this regulatory response is mediated by mRNA stability (Caron et al., 1985; Pachter et al., 1987; Yen et al., 1988). Our results demonstrate that autoregulation of *αTub67C* does not occur in *Drosophila* oocytes and are consistent with a simple linear dose response model. Similar observations have been made by Elizabeth Raff and colleagues (Department of Biology, Indiana University, Bloomington, IN 47405-6801, USA) for β-tubulin in the *Drosophila* testis, where one and two extra copies of the *B2t* tubulin gene result in a 50% and 100% increase, respectively, in accumulation of this β-tubulin protein (personal communication). Until further data are available, the absence of autoregulation in *Drosophila* ovaries and testes can be rationalized as a peculiarity of tissues that store protein and mRNA for future use, in contrast to cells that must meet only immediate cytoskeletal requirements. However, *Saccharomyces cerevisiae*, an organism that might be expected to resemble cultured animal cells in this respect, also fails to fulfil some of the predictions of the autoregulatory model (Katz et al., 1990). Although this yeast does down-regulate tubulin accumulation in response to increased gene dosage, there is no corresponding up-regulatory response when gene dosage is decreased. The relevance of these observations for general mechanisms of tubulin regulation remains to be seen, but they raise the possibility that tubulin autoregulation as understood in cultured cells may not be directly applicable to more complex developmental systems.

We are grateful to Pieter Wensink for providing the *αTub67C* genomic clone, to Mary Lou Pardue for providing the *αTub84B* genomic clone, to Tim Karr for providing the Ax-D5 antibody, and to Elizabeth Raff and William Theurkauf for sharing results prior to publication. This work was supported by a National Science Foundation research grant, number DMB900447, to K. A. M. T. C. K. is an investigator of the Howard Hughes Medical Institute.

REFERENCES

Baker, H. N., Rothwell, S. W., Grasser, W. A., Wallis, K. T. and Murphy, D. B. (1990). Copolymerization of two distinct tubulin isotypes during microtubule assembly in vitro. *J. Cell Biol.* **110**, 97-104.

Ben-Ze'ev, A., Farmer, S. R. and Penman, S. (1979). Mechanisms of regulating tubulin synthesis in cultured mammalian cells. *Cell* **17**, 319-325.

Bo, J. and Wensink, P. C. (1989). The promoter region of the *Drosophila* a2-tubulin gene directs testicular and neural specific expression. *Development* **106**, 581-587.

Bond, J. F., Fridovich-Keil, J. L., Pillus, L., Mulligan, C. R. and Solomon, F. (1986). A chicken-yeast chimeric beta tubulin protein is incorporated into mouse microtubules in vivo. *Cell* **44**, 461-468.

Campos-Ortega, J. A. and Hartenstein, V. (1985). *The Embryonic Development of Drosophila melanogaster*. Berlin: Springer-Verlag.

Caron, J. M., Jones, A. L., Rall, L. B. and Kirschner, M. W. (1985). Autoregulation of tubulin synthesis in enucleated cells. *Nature* **317**, 648-651.

Cassimeris, L., Pryor, N. K. and Salmon, E. D. (1988). Real time observations of microtubule dynamic instability in living cells. *J. Cell Biol.* **107**, 2223-2231.

Church, K., Nicklas, R. B. and Lin, H.-P. P. (1986). Micromanipulated bivalents can trigger mini-spindle formation in *Drosophila melanogaster* spermatocyte cytoplasm. *J. Cell Biol.* **103**, 2765-2773.

Cleveland, D. W. (1989). Autoregulated control of tubulin synthesis in animal cells. *Curr. Opin. Cell Biol.* **1**, 10-14.

Cleveland, D. W., Hwo, S. and Kirschner, M. W. (1977). Purification of tau, a microtubule-associated protein that induces assembly from purified tubulin. *J. Mol. Biol.* **116**, 207-225.

Cleveland, D. W., Lopata, M. A., Sherline, P. and Kirschner, M. W. (1981). Unpolymerized tubulin modulates the level of tubulin mRNAs. *Cell* **25**, 537-546.

Cooper, K. W. (1950). Normal spermatogenesis in *Drosophila*. In *Biology of Drosophila* (ed. M. Demerec), pp. 1-61. New York: Hafner Publishing Co.

Diederich, R. J., Merrill, V. K. L., Pultz, M. A. and Kaufman, T. C. (1989). Isolation, structure and expression of *labial*, a homeotic gene of the Antennapedia Complex involved in *Drosophila* head development. *Genes Dev.* **3**, 399-414.

Doane, W. H. (1960). Completion of meiosis in uninseminated eggs of *Drosophila melanogaster*. *Science* **132**, 677-678.

Drubin, D. G. and Kirschner, M. W. (1986). Tau protein function in living cells. *J. Cell Biol.* **103**, 2739-2746.

Foe, V. E. and Alberts, B. M. (1983). Studies of nuclear and cytoplasmic behaviour during the five mitotic cycles that precede gastrulation in *Drosophila* embryogenesis. *J. Cell. Sci.* **61**, 1-70.

Freeman, M., Nusslein-Volhard, C. and Glover, D. M. (1986). The dissociation of nuclear and centrosomal division in *gnu*, a mutation causing giant nuclei in *Drosophila*. *Cell* **46**, 457-468.

Glover, D. M. (1989). Mitosis in *Drosophila*. *J. Cell Sci.* **92**, 137-146.

Guo, L.-H., Stepien, P., Tso, J. Y., Drousseau, R., Narang, S., Thomas, D. Y. and Wu, R. (1984). Synthesis of human insulin gene. VIII. Construction of expression vectors for fused proinsulin production in *Escherichia coli*. *Gene* **29**, 251-254.

Hays, T. S, Seuring, R., Robertson, B., Prout, M. and Fuller, M. T. (1989). Interacting proteins identified by genetic interactions: a missense mutation in α-tubulin fails to complement alleles of the testis-specific β-tubulin gene of *Drosophila melanogaster*. *Mol. Cell. Biol.* **9**, 875-884.

Horio, T. and Hotani, H. (1986). Visualization of the dynamic instability of individual microtubules by dark field microscopy. *Nature* **321**, 605-607.

Hoyle, H. D. and Raff, E. C. (1990). Two *Drosophila* beta tubulin isoforms are not functionally equivalent. *J. Cell Biol.* **111**, 1009-1026.

Joshi, H. C., Yen, T. J. and Cleveland, D. W. (1987). In vivo coassembly of a divergent beta-tubulin subunit (Cβ6) into microtubules of different function. *J. Cell Biol.* **105**, 2179-2190.

Kalfayan, L. and Wensink, P. C. (1981). α-Tubulin genes of *Drosophila*. *Cell* **24**, 97-106.

Kalfayan, L. and Wensink, P. C. (1982). Developmental regulation of *Drosophila* α-tubulin genes. *Cell* **29**, 91-98.

Karr, T. L. (1991). Intracellular sperm/egg interactions in *Drosophila*: a three-dimensional structural analysis of a paternal product in the developing egg. *Mech. Dev.* **34**, 101-112.

Katz, W., Weinstein, B. and Solomon, F. (1990). Regulation of tubulin levels and microtubule assembly in *Saccharomyces cerevisiae*: Consequences of altered tubulin gene copy number. *Mol. Cell. Biol.* **10**, 5286-5294.

Leicht, B. G. and Bonner, J. J. (1988). Genetic analysis of the chromosomal region 67A-D of *Drosophila melanogaster*. *Genetics* **119**, 579-593.

Lewis, E. B. and Bacher, F. (1968). Method of feeding ethyl methane sulfonate (EMS) to *Drosophila* males. *Dros. Inform. Serv.* **43**, 193.

Lewis, S. A., Wei, G. and Cowan, N. J. (1987). Free intermingling of mammalian β-tubulin isotypes among functionally distinct microtubules. *Cell* **49**, 539-548.

Lewis, S. A., Ivanov, I. E., Lee, G.-H. and Cowan, N. (1989). Organization of microtubules in dendrites and axons is determined by a short hydrophobic zipper in microtubule-associated proteins MAP2 and tau. *Nature* **342**, 498-505.

Lindsley, D. L. and Zimm, G. G. (1992). *The Genome of* Drosophila melanogaster. San Diego: Academic Press.

Lopata, M. A. and Cleveland, D. W. (1987). In vivo microtubules are copolymers of available isotypes: localization of each of six vertebrate β-tubulin isotypes using polyclonal antibodies elicited by synthetic peptide antigens. *J. Cell Biol.* **105**, 1707-1720.

Mahaffey, J. W. and Kaufman, T. C. (1987). Distribution of the *Sex combs reduced* gene products in *Drosophila melanogaster*. *Genetics* **117**, 51-60.

Mahowald, A. P. and Kambysellis, M. P. (1980). Oogenesis. In *The Genetics and Biology of Drosophila*, vol. 2d (eds. M. Ashburner and T. R. F. Wright), pp. 107-224. London: Academic Press.

Mahowald, A. P., Goralski, T. J. and Caulton, J. H. (1983). *In vitro* activation of *Drosophila* eggs. *Dev. Biol.* **98**, 437-445.

Matthews, K. A. and Kaufman, T. C. (1987). Developmental consequences of mutations in the 84B α-tubulin gene of *Drosophila melanogaster*. *Dev. Biol.* **119**, 100-114.

Matthews, K. A., Miller, D. F. B. and Kaufman, T. C. (1989). Developmental distribution of RNA and protein products of the *Drosophila* α-tubulin gene family. *Dev. Biol.* **132**, 45-61.

Matthews, K. A., Miller, D. F. B. and Kaufman, T. C. (1990). Functional implications of the unusual spatial distribution of a minor α-tubulin isotype in *Drosophila*: a common thread among chordotonal ligaments, developing muscle and testis cyst cells. *Dev. Biol.* **137**, 171-183.

Mischke, D. and Pardue, M. L. (1982). Organization and expression of α-tubulin genes in *Drosophila melanogaster*. *J. Mol. Biol.* **156**, 449-466.

Okabe, S. and Hirokawa, N. (1990). Turnover of fluorescently labelled tubulin and actin in the axon. *Nature* **343**, 479-482.

Pachter, J. S., Yen, T. J. and Cleveland, D. W. (1987). Autoregulation of tubulin expression is achieved through specific degradation of polysomal tubulin mRNAs. *Cell* **51**, 283-292.

Pattatucci, A. M. and Kaufman, T. C. (1990). Antibody staining of imaginal discs. In *Drosophila Information Newsletter*, **Vol. 1** (eds. C. Thummel and K. Matthews). Electronic mail publication, DIS-L@IUBVM. UCS. INDIANA. EDU.

Pirrotta, V. (1988). Vectors for P-mediated transformation in *Drosophila*. In *Vectors, A Survey of Molecular Cloning Vectors and Their Uses* (eds. R. L. Rodriguez and D. T. Denhardt), pp. 437-456. Butterworth, Boston.

Rabinowitz, M. (1941). Studies on the cytology and early embryology of the egg of *Drosophila melanogaster*. *J. Morphol.* **69**, 1-49.

Raff, E. C. (1984). Genetics of microtubule systems. *J. Cell Biol.* **99**, 1-10.

Robertson, H. M., Preston, C. R., Phillis, R. W., Johnson-Schlitz, D. M., Benz, W. K. and Engels, W. R. (1988). A stable genomic source of *P* element transposase in *Drosophila melanogaster*. *Genetics* **118**, 461-470.

Savage, C., Hamelin, M., Culotti, J. G., Coulson, A., Albertson, D. G. and Chalfie, M. (1989). *mec-7* is a β-tubulin gene required for the production of 15-protofilament microtubules in *Caenorhabditis elegans*. *Genes Dev.* **3**, 870-881.

Serrano, L., Wandosell, F. and Avila, J. (1986). Location of the regions recognized by five commercial antibodies on the tubulin molecule. *Analyt. Biochem.* **159**, 253-259.

Schatz, P. J., Solomon, F. and Botstein, D. (1986). Genetically essential and nonessential α-tubulin genes specify functionally interchangable proteins. *Mol. Cell. Biol.* **6**, 3722-3733.

Sonnenblick, B. P. (1950). The early embryology of *Drosophila melanogaster*. In *Biology of Drosophila* (ed. M. Demerec), pp. 62-167. New York: Hafner Publishing Co.

Tates, A. D. (1971). *Cytodifferentiation during Spermatogenesis in Drosophila melanogaster*. 'S-Gravenhage: Drukkerij J. H. Pasmans.

Theurkauf, W. E. (1992). Behavior of a structurally divergent α-tubulin isotype during *Drosophila* embryogenesis: Evidence for post-translational regulation of isotype abundance. *Dev. Biol.* **154**, 205-217.

Theurkauf, W. E. and Hawley, R. S. (1992). Meiotic spindle assembly in *Drosophila* females: behavior of nonexchange chromosomes and the effects of mutations in the *nod* kinesin-like protein. *J. Cell Biol.* **116**, 1167-1180.

Theurkauf, W. E., Baum, H., Bo, J. and Wensink, P. C. (1986). Tissue-specific and constitutive α-tubulin genes of *Drosophila melanogaster* code for structurally distinct proteins. *Proc. Natl. Acad. Sci. USA* **83**, 8477-8481.

Theurkauf, W. E., Smiley, S., Wong, M. L. and Alberts, B. M. (1992). Reorganization of the cytoskeleton during *Drosophila* oogenesis: implications for axis specification and intercellular transport. *Development* **115**, 923-936.

Walker, R. A., O'Brien, E. T., Pryer, N. K., Soboeiro, M. F., Voter, W. A., Erickson, H. P. and Salmon, E. D. (1990). Dynamic instability of individual microtubules analyzed by video light microscopy: rate constants and transition frequencies. *J. Cell Biol.* **107**, 1437-1448.

Warn, R. M. and Warn, A. (1986). Microtubule arrays present during the syncytial and cellular blastoderm stages of the early Drosophila embryo. *Exp. Cell Res.* **163**, 201-210.

Yen, T. J., Gay, D. A., Pachter, J. S. and Cleveland, D. W. (1988). Autoregulated changes in stability of polyribosome-bound β-tubulin mRNAs are specified by the first 13 translated nucleotides. *Mol. Cell. Biol.* **8**, 1224-1235.

Zalokar, M. and Erk, I. (1976). Division and migration of nuclei during early embryogenesis of *Drosophila melanogaster*. *J. Microsc. Biol. Cell.* **25**, 97-106.

(Accepted 17 November 1992)